1 **_CFH_ loss in human RPE cells leads to inflammation and complement system**

2 **dysregulation _via_ the NF-ƙB pathway**

3

4 **Running title:** _CFH_ loss leads to NF-κB mediated inflammation

5

6 Angela Armento*[1], Tiziana L Schmidt*[1], Inga Sonntag*, David Merle*, Mohamed Ali

7 Jarboui*, Ellen Kilger*, Simon J. Clark*[†‡]; Marius Ueffing*[†]

8

9 * Institute for Ophthalmic Research, Department for Ophthalmology, Eberhard Karls

10 University of Tübingen, Tübingen, Baden-Württemberg, 72076, Germany

11 † University Eye Clinic, Department for Ophthalmology, Eberhard Karls University of

12 Tübingen, Tübingen, Baden-Württemberg, 72076, Germany

13 ‡ Lydia Becker Institute of Immunology and Inflammation, Faculty of Biology, Medicine and

14 Health, University of Manchester, Manchester, M13 9PT, UK

15
16 corresponding authors:

17 Angela Armento, PhD

18 Institute for Ophthalmic Research, Department for Ophthalmology, Eberhard Karls University

19 of Tübingen, Tübingen, Baden-Württemberg, 72076, Germany

20 angela.armento@uni-tuebingen.de

21 Phone: +49 7071 29 84953

22
23 Marius Ueffing, PhD.

24 Institute for Ophthalmic Research, Department for Ophthalmology, Eberhard Karls University

25 of Tübingen, Tübingen, Baden-Württemberg, 72076, Germany

26 marius.ueffing@uni-tuebingen.de

27

28 [1] These authors contributed equally

29

33 **Abstract**

34 Age-related macular degeneration (AMD), the leading cause of vision loss in the elderly, is a

35 degenerative disease of the macula, where retinal pigment epithelium (RPE) cells are damaged

36 in the early stages of the disease and chronic inflammatory processes may be involved. Besides

37 ageing and lifestyle factors as drivers of AMD, a strong genetic association to AMD is found

38 in genes of the complement system, with a single polymorphism in the complement factor H

39 gene (*CFH*), accounting for the majority of AMD risk. However, the exact mechanism by which

40 *CFH* dysregulation confers such a great risk for AMD and its role in RPE cells homeostasis is

41 unclear. To explore the role of endogenous *CFH* locally in RPE cells, we silenced *CFH* in

42 human hTERT-RPE1 cells. We demonstrate that endogenously expressed *CFH* in RPE cells

43 modulates inflammatory cytokine production and complement regulation, independent of

44 external complement sources or stressors. We show that loss of the factor H protein (FH) results

45 in increased levels of inflammatory mediators (*e.g.* IL-6, IL-8, GM-CSF) and altered levels of

46 complement proteins (*e.g. C3, CFB* upregulation and *C5* downregulation) that are known to

47 play a role in AMD. Moreover, we identified the NF-ƙB pathway as the major pathway involved

48 in the regulation of these inflammatory and complement factors. Our findings suggest that in

49 RPE cells, FH and the NF-ƙB pathway work in synergy to maintain inflammatory and

50 complement balance and in case either one of them is dysregulated, the RPE microenvironment

51 changes towards a pro-inflammatory AMD-like phenotype.

52

53

Introduction

The specific anatomic structure of the human eye permits a tightly regulated local immune response to be sufficient in protecting the retina from external pathogens and to maintain its visual function (1). In immune privileged organs like the eye an excessive immune response, and the subsequent recruitment of circulating immune cells, may lead to tissue damage and affect the function of such a highly specified organ. Ocular immune privilege is mainly ensured by the physical barrier formed by the retinal pigment epithelium (RPE) cell monolayer sitting on an extracellular matrix (ECM), called Bruch´s membrane (BrM), which separates the neurosensory retina from the choroid and choriocapillaris (2). The main advantage of an intact RPE/BrM interface is that it provides an effective barrier for the selectivity of molecular diffusion, especially with regard to a possible systemic inflammatory insult (3). Considering that the composition of BrM relies on the deposition of ECM components from both the endothelium cells of the choriocapillaris and the RPE cells, any disruption to RPE cell homeostasis is deleterious for effective barrier maintenance. Moreover, RPE cells exert several other functions needed for retinal health. RPE cells are not only responsible for the phagocytosis and recycling of photoreceptor outer segments (POS), but they also possess antioxidant activity and actively take up nutrients from, and release discard material into, the BrM (4). Although increased signs of inflammation are observed in several retinal degenerative diseases (5), the combination of RPE cell dysfunction, barrier breakdown and subtle, chronic, inflammation is characteristic for the disease age-related macular degeneration (AMD) (6).

AMD is a progressive degenerative disease of the retina, which leads to patients losing their central vision and, in later stages, suffering blindness (7). AMD affects foremost the elderly population and it is estimated that with increasing life expectancy around 300 million people will be affected by 2040 (8). A hallmark of the disease is the presence of deposits, called drusen, within BrM underneath the RPE cells, which not only impair RPE function but also greatly alter the properties of BrM (9). The events that lead to these changes are not yet fully understood, however it is known that AMD is caused by a combination of ageing, genetic predisposition and lifestyle (10-12). The majority of genetic risk lies in the genes of the alternative pathway of the complement system (13), which is an important part of the innate immune system. The canonical role of the complement system is to recognize and mediate the removal of pathogens, debris and dead cells *via* the activation of the complement proteolytic cascade (14). Clearly, tight regulation of complement activation is required to prevent inflammation-induced tissue damage, especially in an immune privileged organ like the eye (15). At the site of complement activation the release of the cleaved complement factors C3a

88   and C5a, called anaphylatoxins, leads to the recruitment and activation of circulating immune

89   cells such as macrophages and leucocytes (16). Additionally, C3a and C5a activate resident

90   immune cells, like microglia and Muller cells, generating a chronic inflammatory environment,

91   which is observed in AMD (17, 18). Complement dysregulation is not only linked to AMD *via*

92   genetic association. Several complement activation products have also been detected in drusen,

93   as well as in the eyes and in the blood of AMD patients (9, 19, 20). One of the most common

94   genetic risks, accounting for 50% of attributable risk for AMD, corresponds to a polymorphism

95   in the complement factor H (*CFH*) gene that consists of a Tyr to His amino acid substitution at

96   position 402 in the pre-processed factor H protein (FH: position 384 in the mature FH protein)

97   (21, 22). The Y402H polymorphism is also present in the alternative splicing product of the

98   *CFH* gene, the protein called factor H-like protein 1 (FHL-1), which is around a third of the

99   size of FH and found to predominate in BrM (23). FH and FHL-1 are negative regulators of the

100   alternative pathway of the complement system and promote the degradation of C3b, a

101   breakdown product of C3 and the central component of the complement activation

102   amplification loop (24). The AMD high-risk genetic variant *CFH* 402H is believed to be

103   involved in AMD pathogenesis in different ways. Indeed, besides the fact that the FH/FHL-1

104   402H variant has been associated with increased complement activation (25), the same variant

105   also shows reduced binding affinity to ECM components (*e.g.* heparan sulphate) (26), oxidized

106   lipids (*e.g.* malondialdehyde MDA) (27) and inflammatory mediators (*e.g.* C-reactive protein

107   CRP) (28, 29). Most importantly, the function of the FH/FHL-1 proteins may differ depending

108   on their source and location (24, 30). Indeed, in this regard, the endogenous impact of *CFH*

109   proteins in RPE cells has rarely been investigated. In our recent study, we unraveled a non-

110   canonical function of endogenous FH, as the predominant splice form found in RPE cells. By

111   silencing *CFH* in hTERT-RPE1 cells, we showed that FH loss in RPE cells not only modulates

112   the extracellular microenvironment *via* its regulation of C3 levels, but also has an intracellular

113   impact on the antioxidant functions and metabolic homeostasis of RPE cells (31). In the current

114   study, the same model was employed to investigate the endogenous role of FH in the

115   inflammatory response of RPE cells, since RPE cells actively contribute to the maintenance of

116   the immune privileged status of the eye, and not only *via* their barrier function. In particular,

117   we focused on the interactions between FH, inflammation and the nuclear factor kappa-light-

118   chain-enhancer of activated B cells (NF-ƙB) pathway in RPE cells. The NF-ƙB pathway is a

119   known key regulator of inflammation and upon canonical regulation of this pathway, the p65

120   subunit (RelA) of the NF-ƙB complex is phosphorylated and translocates to the nucleus, where

121   it promotes the transcription of several NF-ƙB target genes, including inflammatory cytokines,

4

122   chemokines and also genes involved oxidative stress response (32). Activation of the NF-ƙB
123   pathway has been associated with several neurodegenerative diseases, including Alzheimer's
124   and Parkinson's disease (33), but also in retinal degenerative diseases, such as diabetic
125   retinopathy (34).

126   Here, we show that RPE cells are immunocompetent with respect to their ability to
127   express and regulate immune-modulatory genes including cytokines and chemokines. FH loss
128   results in an increase of inflammatory cytokines and chemokines in an NF-ƙB dependent
129   fashion. Moreover, we discovered that FH loss strongly alters the regulation of other
130   complement genes, again in an NF-ƙB dependent way, thereby creating a dysfunction in
131   complement pathway regulation. As such, the NF-ƙB pathway emerged as a major signaling
132   pathway controlling immune competence and response in RPE cells.

133

Material and Methods

Cell culture and experimental settings

The human RPE cell line hTERT-RPE1 was obtained from the American Type Culture Collection (ATCC). Cells were maintained in Dulbecco's modified Eagle's medium (DMEM; Gibco, Germany) containing 10% fetal calf serum (FCS; Gibco, Germany), penicillin (100 U/ml), streptomycin (100 µg/ml) in a humidified atmosphere containing 5% CO_2. Cells were seeded in complete growth medium without phenol red in 12-well plates and allowed to attach overnight. Gene silencing was performed with Viromer Blue reagent according to the manufacturer's instructions (Lipocalyx, Germany). Culture medium was substituted with fresh medium and siRNA mixture was added dropwise. We employed a mix of three different double strand hairpin interference RNAs specific for either *CFH* or *RELA* and a negative control (Neg), recommended by the provider (IDT technologies, Belgium). In experiments where double silencing was required (siCFH + siRELA), an additional amount of siNeg siRNA was added in the single silencing samples (siNeg, siRELA and siCFH) to keep equal concentrations. Cells were then maintained in serum free medium for the indicated time and where indicated, medium was supplemented with FH (1 µg/ml), C3 (0.1 µg/ml) or C3b (0.1 µg/ml) (CompTech, Texas, USA) for 48 or 144 hours (h).

RNA extraction, cDNA synthesis and quantitative RT-PCR

At the indicated time points, total RNA was extracted with PureZOL reagent, according to the manufacturer's instructions (Bio-Rad Laboratories, USA) and cDNA was synthesized *via* reverse-transcription of 1 µg of RNA using M-MLV Reverse Transcriptase (Promega (Wisconsin, USA). cDNA was used to analyse differences in gene expression by qRT-PCR employing iTaq Universal SYBR Green Supermix (Bio-Rad Laboratories, USA) along with gene specific forward and reverse primers (10 µM) listed in Table 1. PCR protocol includes 40 cycles of: 95°C (5 seconds) and 57°C (30 seconds), carried on CFX96 Real-Time System (Bio-Rad Laboratories, USA). Relative mRNA expression of each gene of interest (GOI, Table I) was quantified using 60S acidic ribosomal protein P0 (PRLP0) as the housekeeping control gene.

Table I. List of primers used in this study

Target gene	Forward primer	Reverse Primer
CFH	5´ CTG ATC GCA AGA AAG ACC AGT A 3´	5´ TGG TAG CAC TGA ACG GAA TTA G 3´
CFB	5´ GCT GTG AGA GAG ATG CTC AAT A 3´	5´ GAC TCA CTC CAG TAC AAA G 3´

C3	5´ ACG GCC TTT GTT CTC ATC TC 3´	5´ CAA GGA AGT CTC CTG CTT TAG T 3´
C5	5´ CGA TGG AGC CTG CGT TAA TA 3´	5´ CTT GCG ACG ACA CAA CAT TC 3´
CFI	5`- TAC TCA CCT CTC CTG CGA TAA- 3´	5`- GGG CAC TGA TAC GGT AGT TTA C -3`
CCL2	5´ GGC TGA GAC TAA CCC AGA AAC 3`	5´ GAA TGA AGG TGG CTG CTA TGA 3`
IL6	5´ CCA GGA GAA GAT TCC AAA GAT GTA 3´	5´ CGT CGA GGA TGT ACC GAA TTT 3´
CXCL8	5´ AAA TCT GGC AAC CCT AGT CTG 3´	5´ GTG AGG TAA GAT GGT GGC TAA T 3´
RELA	5´ CTG TCC TTT CTC ATC CCA TCT T 3´	5´ TCC TCT TTC TGC ACC TTG TC 3´
PRLP0	5´ GGA GAA ACT GCT GCC TCA TAT C 3´	5´ CAG CAG CTG GCA CCT TAT T 3´

165

Western Blotting

Protein expression was analyzed in both cell lysates and cell supernatants. After debris removal, cell culture supernatants were precipitated with ice-cold acetone. For protein analysis of cell lysates, cells were lysed in Pierce IP Lysis Buffer, containing Halt Protease & Phosphatase Inhibitor (Thermo Fisher, Massachusetts, USA). Protein concentrations were determined with the Bradford quantification assay, using BSA as a standard. Equal amounts of cell lysates or equal volumes of cell supernatants were prepared in NuPAGE LDS Sample Buffer, containing reducing agent (Thermo Fisher, Massachusetts, USA) and analyzed on Novex 8-16% Tris-Glycine gels (Invitrogen, California, USA). Subsequently proteins were transferred onto PVFD membranes and western blot detection carried out as previously described (31), using the primary antibodies listed in Table II. Pictures were acquired with a FusionFX imaging system (Vilber Lourmat, France) and the intensity density of individual bands was quantified using the ImageJ software.

Table II. List of primary antibodies used in this study

Antibody	Supplier	Number	
β-actin	Cell Signaling	#3700	182
Complement C3	Invitrogen, ThermoFisher	#PA5-21349	183
Factor H (FH)	SantaCruz Biotechnology	sc-166608	184
p-NF-kB p65	Cell Signaling	#3033	185
Total NF-kB p65	Cell Signaling	#8242	186

C3b ELISA

C3/C3b ELISA to evaluate the concentration of C3/C3b in cell culture supernatants was performed according to the manufacturer´s instructions (Abcam, UK). Samples and standard controls were loaded in 96 well-plates coated with specific C3b antibody. Absorbance was read

7

193   at a wavelength of 450 nm immediately after the assay procedure using a Spark multimode

194   microplate reader (Tecan, Switzerland). Subtraction readings at 570 nm were taken to correct

195   optical imperfections.

196

197   **Cytokine array**

198   The Proteome Profiler Human Cytokine Array Kit (R&D Systems, Minnesota, USA) was

199   employed to determine the relative levels of 36 different cytokines and the assay was performed

200   according to the manufacturer's instructions. Briefly, the membranes were blocked for 1 h at

201   room temperature. The cellular supernatant samples were further prepared by mixing 400 μl of

202   the sample with 500 μl Array Buffer 4, 600 μl Array Buffer 5 and 15 μl of Detection Antibody

203   Cocktail and incubated for 1 h at room temperature. The prepared mixture was added to the

204   membranes, followed by an incubation period overnight at 4°C. The membranes were washed

205   3 x 10 minutes, incubated in diluted HRP-Streptavidin (1:2000) for 30 minutes, and washed

206   again for 3 x 10 minutes. The Chemi Reagent Mix (1:1 ratio) was dropped onto the membranes,

207   incubated for 1 minute, and the signal was detected by FusionFX (Vilber Lourmat, France) in

208   the automatic mode and, additionally, in an individual programmed mode with an increasing

209   detection time of: 0.5, 1, 1.5, 2, 4, 6, 10 minutes. The results were evaluated with the Fusion

210   software and ImageJ by measuring the intensity density.

211

212   **Bioinformatic analyses**

213   Data analysis of the raw values from the cytokine array as obtained and measured using ImageJ,

214   were normalized to the positive control. For principal component analysis (PCA), values were

215   Pareto scaled by dividing each variable by the square root of the standard deviation to minimize

216   the effect of small noisy variables.

217   The Variable Importance in Projection (VIP) in a Partial Least Square Discriminant

218   Analysis (PLS-DA) was used to identify the most discriminative cytokines for each biological

219   group following siRNA treatment. Similar to the PCA analysis and normalized to the positive

220   control, Pareto scaled values were used. PCA and VIP score analysis were carried out using the

221   R package MetaboAnalystR, integrated in the publicly available platform for statistical analysis

222   metaboanalyst.ca (35).

223

224   **Statistical analysis**

225   The data are presented as mean with the standard error of the mean (SEM) and were generated

226   and tested for their significance with GraphPad Prism 8 software. All data sets were tested for

227   normal distribution, assessed with Shapiro-Wilk normality test. Depending on normal

228   distribution and the parameters to be compared the following tests were performed: Mann-

229   Whitney test was used in case of non-normal distribution, unpaired student´s t-test was used to

230   compare siNeg vs either siCFH or siRELA condition and to compare siCFH vs siCFH +

231   siRELA. Ratio paired t-test was used to compare the relative changes between siCFH vs

232   siCFH+siRELA and siCFH vs siCFH treated (FH, C3 or C3b), only when both conditions were

233   normalized to siNeg control. Values were considered significant with $p < 0.05$.

234

Results

CFH loss leads to upregulation of C3 and inflammatory cytokines in RPE cells

In our previous study, we used siRNA silencing of the *CFH* gene to investigate the impact of reduced FH levels and activity in hTERT-RPE1 cells in response to oxidative stress after 48h *in vitro* (31). Here, we used the same model to investigate immune reactivity of RPE cells after *CFH* knockdown and prolonged its silencing period up to 6 days (144h). In this way, we were able to mimic features of an early stage of AMD where the barrier function of RPE cells remains intact, and therefore the protein composition of the retinal microenvironment depends mostly on RPE cells protein production. Using both the short (48h) and the prolonged (144h) silencing period, we investigated the impact of endogenous FH loss on pro-inflammatory cytokine production and on complement system regulation.

Efficient *CFH* silencing after 48h was already shown before and reproduced in this study (31). Here, we show that also after 144h *CFH* mRNA was significantly reduced in *CFH* knock-down (siCFH) RPE cells compared to control cells (siNeg). The silencing efficiency of almost 90% after 48h was maintained also at 144h (Fig. 1a). Likewise, FH protein levels remained almost undetectable in cell culture supernatants of siCFH cells after 144h (Fig. 1b). With prolonged FH loss, *C3* gene expression (Fig. 1e) and C3 protein levels (Fig. 1c-d) increased significantly. Levels of *C3* mRNA were found to be 20-fold higher in siCFH cells at both time points (Fig. 1e). Similarly, protein levels of secreted C3 were significantly elevated in siCFH cells, as shown by a 2-fold increase in C3/C3b ELISA (Fig. 1c) and a 4-fold increase in C3/C3b alpha and beta chains in Western Blot (Fig. 1d).

Given that early AMD is hallmarked by persistent inflammation (36, 37), we investigated the levels of relevant inflammatory cytokines, including: interleukin-6 (IL6), C-C Motif Chemokine Ligand 2 (CCL2) and interleukin-8 (CXCL8). When FH was downregulated in siCFH cells, we observed an upregulation of IL6 (3-fold at 48h and 2-fold at 144h) and CCL2 (2-fold at 48 and 2.5-fold at 144h) (Fig. 1f-g). Moreover, CXCL8 levels were 8-fold upregulated in siCFH cells, significantly after 48h (Fig. 1h). This indicates that reduction of FH levels and activity in RPE cells leads to an upregulation of relevant pro-inflammatory molecules.

10
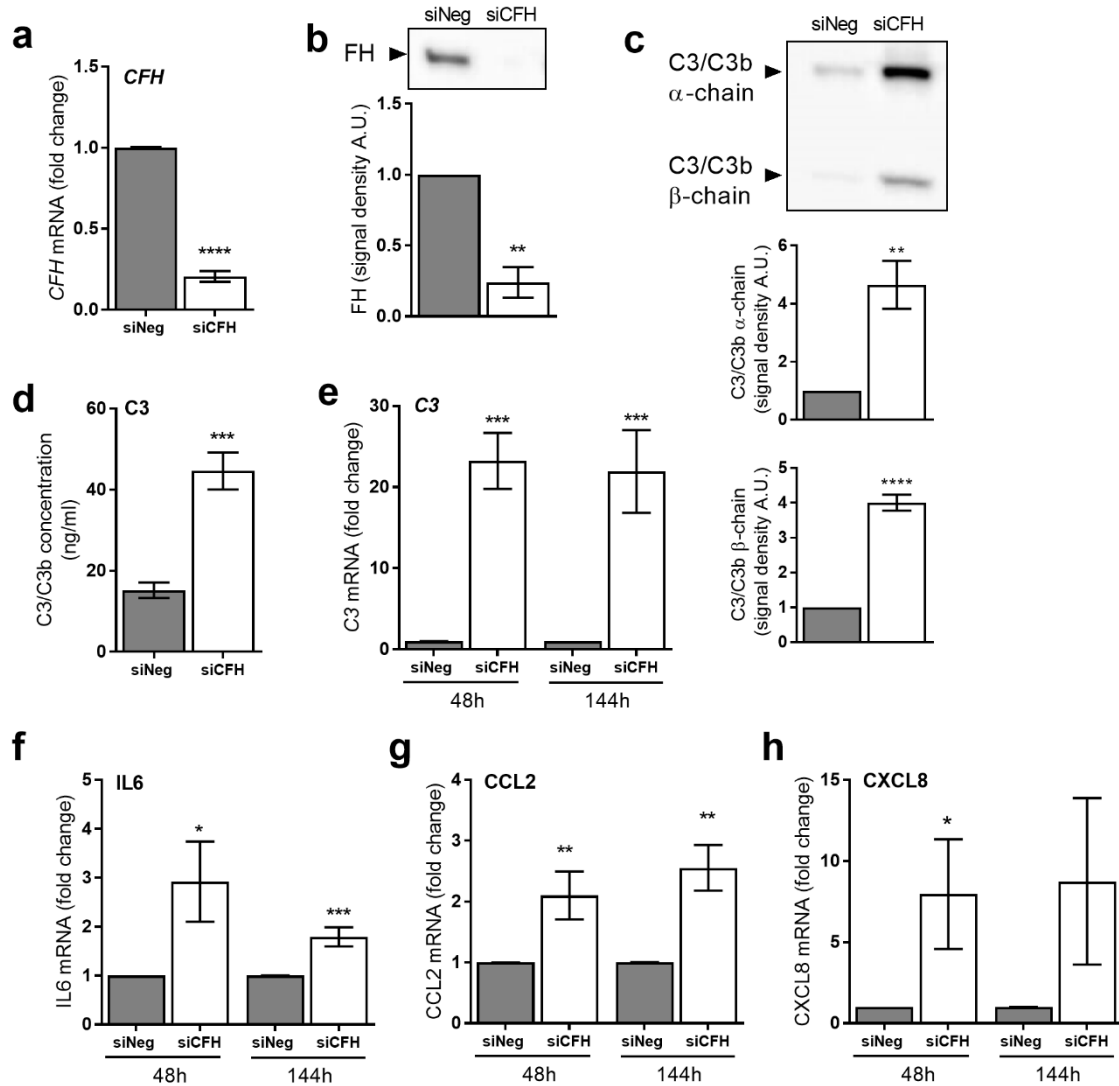
Figure 1. Short and sustained FH reduction leads to increased expression levels of C3 and inflammatory cytokines. hTERT-RPE1 cells were seeded, left to attach overnight and silenced for 24 hours with negative control (siNeg) or *CFH* specific (si*CFH*) siRNA. Afterwards, cells were kept in serum-free medium (SFM) and cell pellets and cell culture supernatants were collected after 48 and 144 hours. **a** Evaluation of *CFH* expression after 144h by qRT-PCR analyses. Data are normalized to the housekeeping gene PRLP0 using Δ ΔCt methods. SEM is shown, n=5. **b** Western blot analyses of FH protein levels in cell culture supernatants of hTERT-RPE1 cells after 144h. Quantification of signal density of 3 independent experiments is shown. **c** Western blot analyses of C3/C3b α-chain and β-chain protein levels in cell culture supernatants of hTERT-RPE1 cells after 144h. Quantification of signal density of 5 independent experiments is shown. **d** C3/C3b ELISA analyses of cell culture supernatants of hTERT-RPE1 cells after 144h. SEM is shown, n=6. **e-h** Monitoring of gene expression by qRT-PCR analyses in hTERT-RPE1 cells: **e** complement component 3 (*C3*), **f** interleukin-6 (IL6), **g** C-C Motif Chemokine Ligand 2 (CCL2) and **h** interleukin-8 (CXCL8). Data are normalized to housekeeping gene PRPL0 using Δ ΔCt method. SEM is shown, n=5-8. Western Blot images were cropped, and full-length blots are presented in Supplementary Fig. S1. Significance was assessed by Student's t-test. *$p<0.05$, **$p<0.01$, *** $p<0.001$, ****$p<0.0001$.

11

**Cytokine expression mediated by FH loss is driven by NF-ƙB activity**

Changes in RPE gene expression after FH reduction, suggests that a pro-inflammatory pathway may be regulated by FH in RPE cells. As NF-ƙB plays a major role in regulating a variety of cytokine expression levels (38), we next investigated if the activity of NF-ƙB was changed by *CFH* silencing. To do so, we monitored the levels of the activated phosphorylated form of the NF-ƙB p65 subunit and its total levels in siNeg and siCFH RPE cells over time (Fig. 2a). We found a dramatic and sustained increase in the activation levels of NF-ƙB, as shown by the increased relative ratio of phosphorylated/total NF-ƙB p65 subunit (Fig. 2b).

To investigate a potential direct correlation between reduced FH activity and the observed NF-ƙB pathway activation, we employed concomitant double silencing of *CFH* and RELA, the gene coding for the NF-ƙB p65 subunit. First, RELA silencing efficiently reduced the levels of the gene by about 90% in siRELA and siCFH + siRELA cells (Fig. 2c). *CFH* silencing had no impact on the expression level of RELA (Fig. 2c). In RELA silenced cells, the protein levels of NF-ƙB p65 were also greatly reduced (Fig. 2d). Quantification of protein levels for both the phosphorylated form of NF-ƙB p65 (Fig. 2e) and total NF-ƙB p65 (Fig. 2f) in siRELA and siCFH + siRELA cells show a significant reduction of protein abundance.

Next, we evaluated gene expression levels of the identified upregulated cytokines in response to RELA silencing. Interestingly, we found that under control conditions (*i.e.* in the presence of FH), the NF-ƙB pathway regulates the expression of CCL2 and CXCL8, but not that of IL6 (Fig. 2g-i). As shown in Fig. 2g, IL6 levels only rise in the absence of FH activity (siCFH). Conversely, a downregulation of NF-ƙB p65 in siCFH cells (siCFH + siRELA), lowers the gene expression of all three cytokines back to basal levels (Fig. 2g-i). In particular, a strong significant reduction was observed for IL6 (Fig. 2g), CXCL8 (Fig. 2i) and for CCL2 (Fig. 2h).

Next, we tested whether exogenous application of FH could revert the effects of endogenous siRNA-based *CFH* suppression on both NF-ƙB activation as well as the expression of inflammatory cytokines. At the same time, we evaluated the effects of an addition of C3 and C3b. The addition of exogenous complement factors, however, did not change NF-ƙB activation levels (Suppl. Fig. S4a-b) nor gene expression levels of IL6 (Suppl. Fig. S4c) and CCL2 (Suppl. Fig. S4d) at any of the time points tested (48h and 144h).
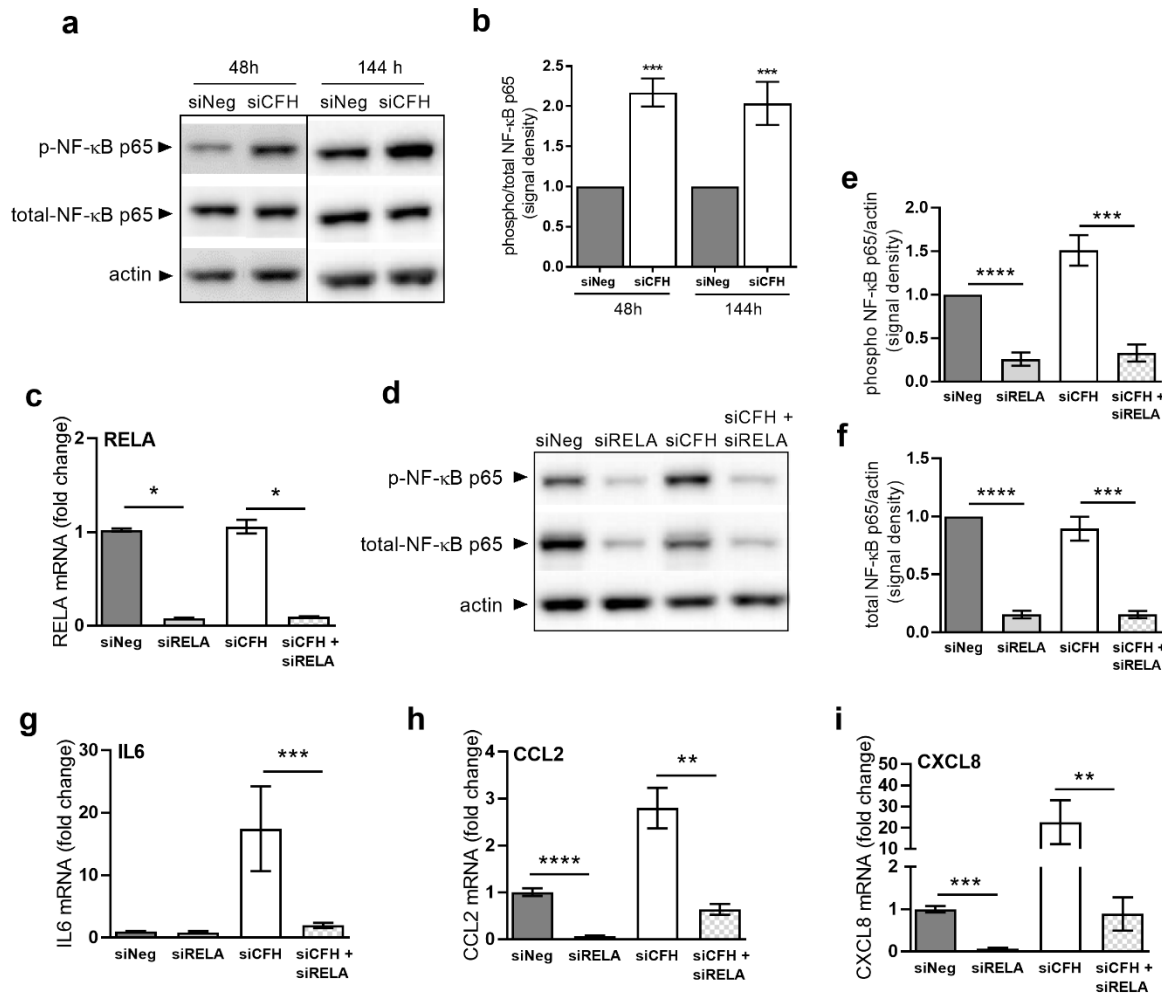
Figure 2. RPE cells deprived of FH show NF-ƙB activation and blocking NF-ƙB abolishes the effects of FH loss on cytokine gene expression levels. hTERT-RPE1 cells were seeded, left to attach overnight and silenced for 24 hours with either negative control (siNeg), *CFH* specific (si*CFH*) or NFƙB/*RELA* specific (siRELA) siRNA or with a combination of siCFH and siRELA siRNA. Afterwards, cells were kept in serum-free medium (SFM) and cell pellets and cell culture supernatants were collected after 48 and/or 144 hours. **a** Western blot analyses of phosphorylated and total levels of p65 NF-ƙB subunit in cell lysates of hTERT-RPE1 cells after 48h and144h. Total actin was used as loading control. **b** Quantification of signal density of at least 4 independent experiments as reported in a. Bars indicate the signal density ratio between levels of phosphorylated and total p65 NFƙB subunit. **c** Evaluation of RELA gene expression levels by qRT-PCR analyses in hTERT-RPE1 cells after 48h. Data are normalized to the housekeeping gene PRPL0 using Δ ΔCt methods. SEM is shown, n=5. **d** Western blot analyses of phosphorylated and total levels of p65 NFƙB subunit in cell lysates of hTERT-RPE1 cells after 48h. Total actin was used as loading control. **e** Quantification of signal density of 3 independent experiments in the conditions reported in c-d. Bars indicate the signal density ratio between phosphorylated p65 NFƙB subunit and actin. **f** Quantification of signal density of 3 independent experiments in the conditions reported in c-d. Bars indicate the signal density ratio between total p65 NFƙB subunit and actin. **g-i** Gene expression analyses by qRT-PCR of hTERT-RPE1 cells in the conditions reported in c-d: **g** interleukin-6 (IL6), **h** C-C Motif Chemokine Ligand 2 (CCL2) and **i** interleukin-8 (CXCL8). Data are normalized to housekeeping gene PRLP0 using Δ ΔCt method. SEM is shown, n=3-5. Western Blot images

13

332   were cropped, and full-length blots are presented in Supplementary Fig. S2-3. Significance was
333   assessed by Student's t-test. *p<0.05, **p<0.01, *** p<0.001, ****p<0.0001.

334

335   In order to assess whether the changes in gene transcription would translate into an
336   inflammatory microenvironment outside of the RPE cells, we monitored the levels of secreted
337   inflammatory factors *via* a cytokine array analyzing the serum free conditioned medium
338   supernatant of hTERT-RPE1 cells after 48 hours (Fig. 3a).

339   Using PCA analysis, we plotted all the signal intensities for each cytokine from all the
340   biological replicates of each group: siNeg, siCFH and siCFH+siRELA. As shown in Fig. 3b,
341   there is clear segregation between siNeg and siCFH as they cluster apart according to the first
342   principal component (PC1), thus indicating a clear effect of siCFH silencing on the RPE
343   cytokine signature. The combination of siCFH + siRELA had little effect on the cytokine profile
344   signature as siCFH + siRELA group cluster tightly with siNeg control (Fig. 3b). This suggests
345   that downregulation of NF-ƙB p65 (siRELA) in siCFH silenced RPE cells results in a reversion
346   of the pro-inflammatory phenotype to normal para-inflammatory homeostasis. As the
347   microarray used for analysis only covers a limited number of cytokines and their relative
348   quantification was based on differences in signal detection after blotting, we chose to use a
349   more supervised approach. Variable Importance in Projection (VIP) values from Partial Least
350   Square Discriminant Analysis (PLS-DA) was used to gain a quantitative estimation of the
351   discriminatory power of each individual cytokine (Fig. 3c). VIP score analysis detected 12
352   cytokines that significantly differentiated between the 3 siRNA groups. IL-8 and IL-6, also
353   shown in Fig. 3d and Fig 3e are the 2 cytokines that contribute the most to the segregation
354   between siNeg, siCFH and siCFH + siRELA. Besides these two, most of the cytokines analysed
355   on the array were increased in the siCFH group when compared to the siNeg controls: colony
356   stimulating factor 2 (GM-CSF, Fig. 3f), serpin family E member 1 (Serpin E1, Fig. 3g), C-X-
357   C Motif Chemokine Ligand 1 (CXCL1/GROα, Fig. 3h), C-C motif chemokine ligand 3 and 4
358   (MIP-1α/-1β, Suppl. Fig. S6a), while the effects on MCP-1, IL18 and IL-1a were less
359   pronounced and only slightly changed (Fig. 3i). Most of these cytokines exhibit a decreased
360   level of abundance when silencing of FH (siCFH) and NF-ƙB p65 (siRELA) was combined:
361   IL-8 (Fig. 3d), IL-6 (Fig. 3e), GM-CSF (Fig. 3f), Serpin E1 (Fig. 3g), CXCL1/GROα were
362   reduced to a base level indicating that an inhibition of the NF-ƙB pathway can dampen or
363   abrogate the consequences of FH loss (Fig. 3h).

364   An exception to this pattern was seen with interleukin 1 receptor antagonist (IL-1Ra,
365   (Fig 3a, c, and Suppl. Fig. S6b), which antagonizes the inflammatory effects of IL-1α/-1β *via*
366   competitive binding to their receptors. The upregulation of IL-1Ra as an anti-inflammatory
367   cytokine suggests that its expression is negatively regulated by NF-ƙB pathway activity.
368   Minimal differences were observed in between the conditions (Suppl. Fig. S6) for macrophage

15

369   migration inhibitory factor (MIF), interleukin-1 alpha (IL-1a), and interleukin-18 (IL-18) and

370   interleukin-21 (IL-21), although the latter was slightly reduced in response to siRELA.

371
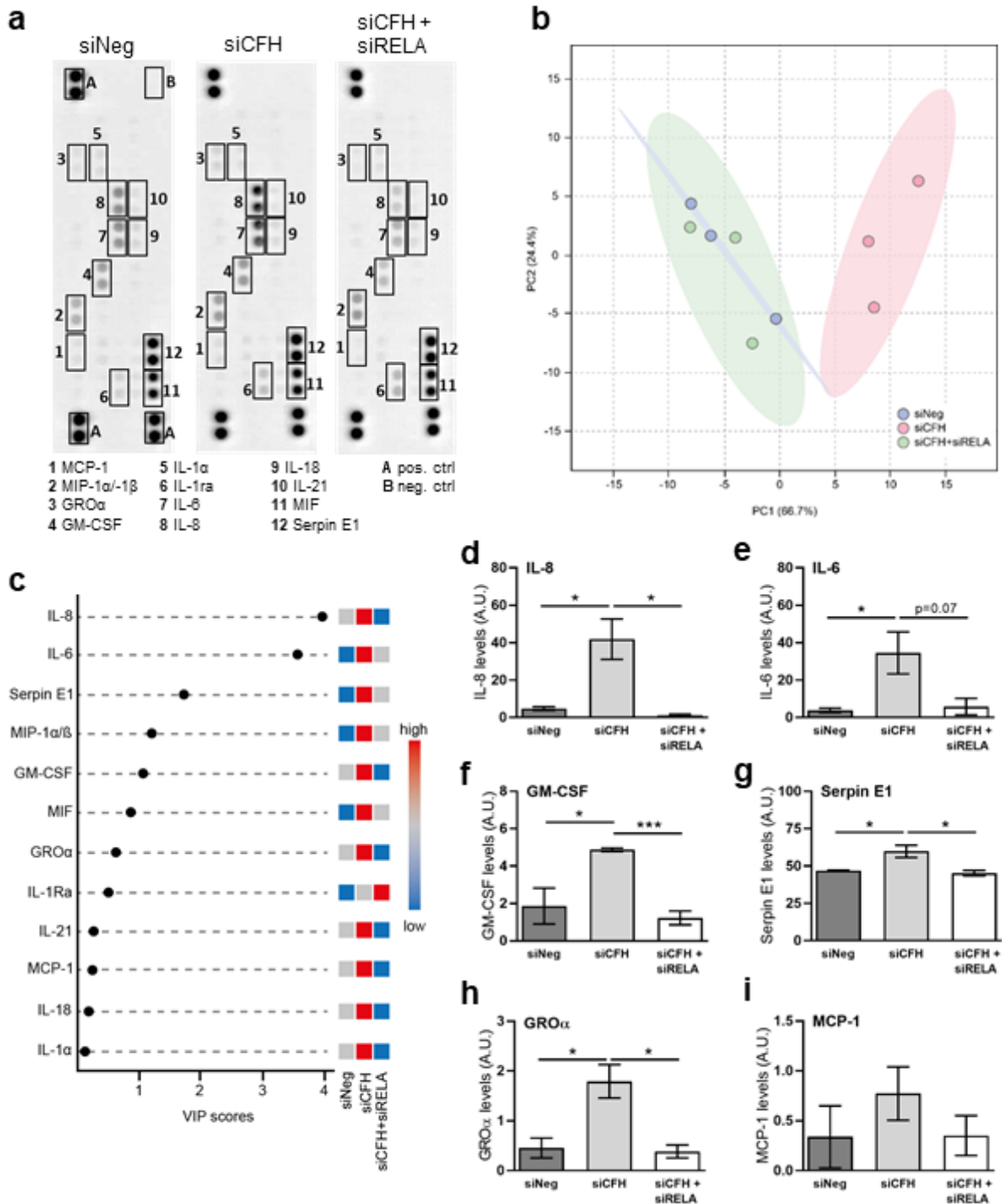
Figure 3. Blockade of NFƙB abolishes the effects of FH loss on secreted cytokines. hTERT-RPE1 cells were seeded, left to attach overnight and silenced for 24 hours with either negative control (siNeg), *CFH* specific (si*CFH*) or with a combination of siCFH and NFƙB/RELA specific (siRELA) siRNA. Afterwards, cells were kept in serum-free medium (SFM) and cell culture supernatants were collected after 48h. **a** Representative image of a Proteome Profiler Human Cytokine Array analysis performed on cell culture supernatants collected from hTERT-RPE1 cells after 48h. **b** PCA Analysis of the Cytokine array data for all biological replicates, samples were colored according to the corresponding siRNA treatment group, 95% confidence regions were plotted and colored according to each group. **c** Variable importance in projection (VIP) score plot derived from PLS-DA analysis, the top cytokines that contribute to the

17

382   segregation between the groups were plotted and their differential abundance was color scaled

383   according to their enrichment (red), depletion (blue), or unchanged (grey).

384   **d-i** Quantification of signal density in the conditions reported in a: **d** interleukin-8, IL-8; **e**

385   interleukin-6, IL-6; **f** colony stimulating factor 2, GM-CSF; **g** serpin family E member 1, Serpin

386   E1; **h** C-X-C Motif Chemokine Ligand 1, CXCL1/GROα; **i** C-C Motif Chemokine Ligand

387   2,CCL2. SEM is shown. n=3. Significance was assessed by Student's t-test. *p<0.05, **p<0.01,

388   *** p<0.001).

389

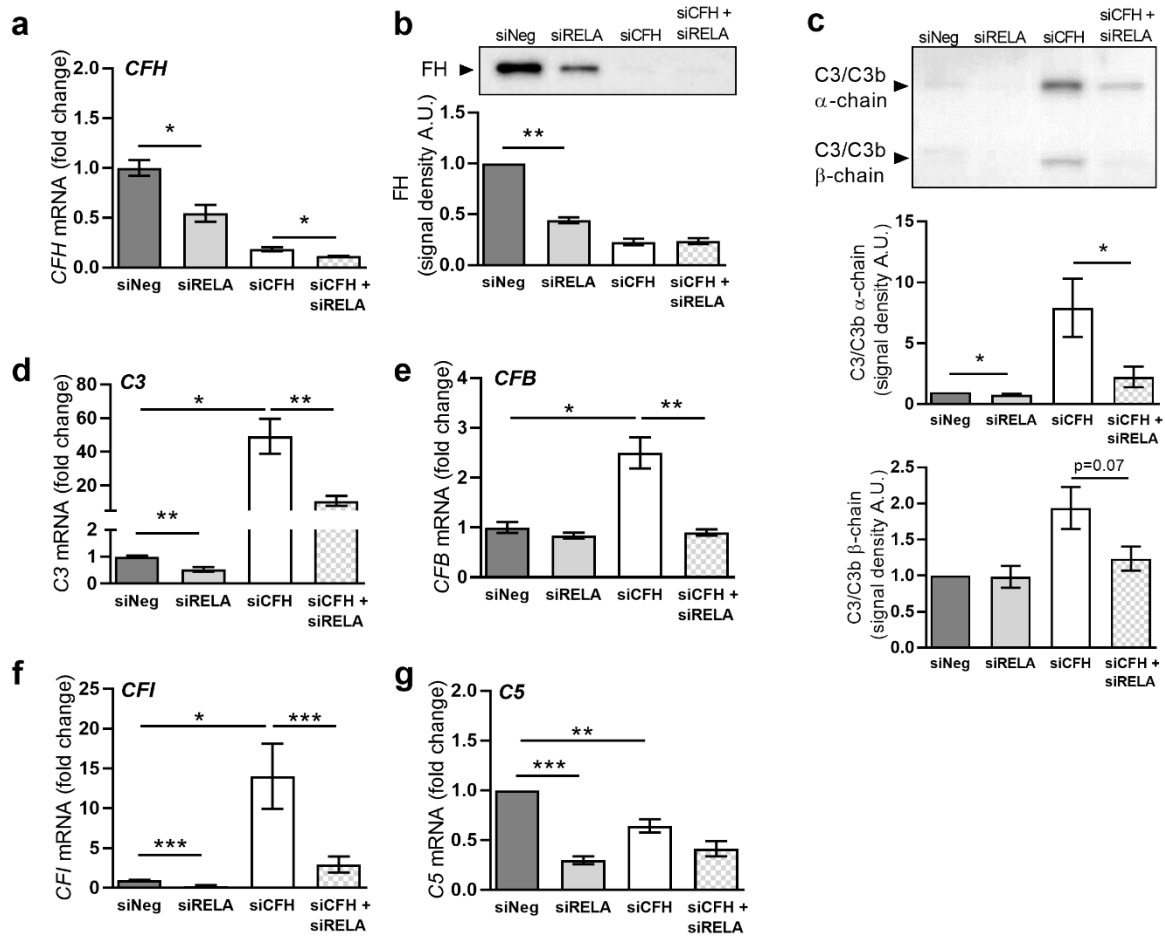**FH loss alters transcription of complement genes *via* the NF-ƙB pathway**

390 The transcriptional regulation of complement genes has remained poorly understood in RPE

392 cells, as well as in general. After finding that reduction of FH activity resulted in a marked

393 upregulation of C3 expression (Fig. 1), we investigated whether either suppression of FH

394 expression or NF-ƙB activity would regulate the expression levels of additional complement

395 factors or regulators.

396 We observed a significant reduction of *CFH* mRNA levels in siRELA cells (Fig. 4a),

397 followed by reduced levels of FH at the protein level (Fig. 4b). C3 levels were also reduced in

398 siRELA cells, both at the protein level (Fig. 4c) as well as RNA level (Fig. 4d). Addition of

399 exogenous FH could only partially revert the effects of endogenous *CFH* silencing on *C3*

400 mRNA levels (Suppl. Fig. S8a) and C3 secreted levels (Suppl. Fig. S8b) after 144h of

401 incubation. Supplementation with C3 and C3b had no impact (Suppl. Fig. 8a) at any time point.

402 Subsequently, we investigated the gene expression levels of *CFB*, an important positive

403 regulator of the alternative pathway of the complement system. We found a significant 2.5-fold

404 increase in the *CFB* gene after *CFH* silencing and a return to basal levels after silencing NF-ƙB

405 p65, while *CFB* levels were not affected by siRELA alone (Fig. 4e). Addition of exogenous FH

406 could only partially revert the effects of endogenous *CFH* silencing on *CFB* mRNA levels,

407 while addition of C3 and C3b had no effects (Suppl. Fig. S8c). Next, we evaluated the

408 expression of *CFI*, a negative regulator of the complement activation in the presence of FH as

409 a co-factor. The RNA levels of *CFI* were 12-fold higher in siCFH cells and were significantly

410 reduced in siRELA cells. (Fig. 4f). Furthermore, we analysed the expression of *C5,* another

411 major component of the complement cascade. The levels of *C5* RNA (Fig. 4g) were reduced

412 by both silencing FH expression in siCFH cells as well as after NF-ƙB p65 silencing in siRELA

413 cells.

414 Most importantly, all factors belonging to the complement system, whose levels were

415 increased in the absence of FH, were reduced *via* suppression of NF-ƙB activity. Thus, *CFB*

416 RNA levels were redirected to basal levels (Fig. 4e); as well as a clear reduction of *CFI* RNA

417 levels was observed (Fig. 4f). *C3* RNA levels were significantly reduced by half (Fig. 4b) and

418 C3 secreted protein levels were also significantly reduced (Fig. 4c).

419

Figure 4. FH loss alters gene transcription of complement system genes *via* the NFƙB pathway. hTERT-RPE1 cells were seeded, left to attach overnight and silenced for 24 hours with either negative control (siNeg), *CFH* specific (si*CFH*), NFƙB/RELA specific (siRELA) siRNA or with a combination of siCFH and siRELA siRNA. Afterwards, cells were kept in serum-free medium (SFM) and cell pellets and cell culture supernatants were collected for after 48h. **a** Evaluation of *CFH* expression by qRT-PCR analyses. Data are normalized to the housekeeping gene PRPL0 using Δ ΔCt methods. SEM is shown, n=5. **b** Evaluation of *C3* expression by qRT-PCR analyses. Data are normalized to the housekeeping gene PRPL0 using Δ ΔCt methods. SEM is shown, n=5. **c** Western blot analyses of C3 α-chain and β-chain protein levels in cell culture supernatants. Quantification of signal density of 4 independent experiments is shown. **d** Western blot analyses of FH protein levels in cell culture supernatants. Quantification of signal density of 3 independent experiments is shown. **e** Evaluation of *CFB* expression by qRT-PCR analyses. Data are normalized to the housekeeping gene PRPL0 using Δ ΔCt methods. SEM is shown, n=5. Western Blot images were cropped, and full-length blots are presented in Supplementary Fig. S7. Significance was assessed by Student's t-test. *p<0.05, **p<0.01.

20

Discussion

Given the strong association of the *CFH* gene with AMD, and a clear role of RPE cells in maintaining homeostasis in the retinal microenvironment, we investigated the role of FH in RPE cells with respect to its impact on balancing molecular mechanisms of inflammation. Here, we demonstrate that endogenously expressed *CFH* in RPE cells modulates inflammatory cytokine production and complement regulation, independent of external complement sources or stressors. We show that decreased *CFH* levels and activity result in increased levels of inflammatory cytokines, chemokines and growth factors, that are known to play a role in AMD, as well as several other neurodegenerative diseases. Although our study reported here does not delineate between the two protein products made by the *CFH* gene (*i.e.* FH and FHL-1) it is reasonable to assume that given FH is the major splice variant expressed by hTERT-RPE1 cells (see Fig. S1) that the biological consequences of *CFH* gene silencing in our study are mediated primarily by FH.

Based on the levels of secreted inflammatory proteins and PCA analysis (Fig. 3), we observed a clear segregation between control RPE cells (siNeg) and RPE cells deprived of *CFH*. The main discriminatory factors were IL-6 and IL-8, which were also the most upregulated cytokines after *CFH* silencing. Besides their role in inflammation, IL-6 and IL-8 are both members of the senescence-associated secretory pathway (SASP) and involved in ageing processes. Indeed, H_2O_2-mediated senescence in ARPE19 cells leads to increased levels of IL-6 and IL-8 when FH levels were reduced (39). Moreover, increased systemic IL-6 levels were found in patients with AMD, mostly in relation to the late subtypes of the disease (40). Interestingly, a study exploring potential new drug targets for AMD identified IL-6 as a candidate target (41).

We found in RPE cells lacking FH increased secreted levels of GM-CSF (Fig. 3), a growth factor that promotes activation and survival of microglia cells and macrophages (42). Interestingly, GM-CSF levels have been found to be elevated in the vitreous of postmortem human eyes genotyped for the *CFH* Y402H SNP, and in parallel accumulation of choroidal macrophages was observed (43). In this study, local accumulation of GM-CSF was found after stimulation with the anaphylatoxins C3a and C5a (43). Our data suggest that RPE cells may be a source of GM-CSF found in the *CFH* Y402H post-mortem eye.

Serpin E1, also known as Plasminogen Activator Inhibitor-1 (PAI-1), was upregulated in siCFH RPE cells. Serpin E1 is involved in ECM remodeling and angiogenesis (44), processes that are altered at the Bruch´s membrane/choroid interface in AMD (2). Serpin E1 is also considered a senescence marker in several tissues (44). High levels of Serpin E1 have been

21

470   associated with neovascularization in AMD and diabetic retinopathy (45). Serpin E1 mediates

471   some of its effects *via* binding to the α5β3 integrin (46)*,* and interestingly also FH and its

472   truncated form FHL-1 modulate RPE function *via* binding a closely related integrin, α5β1 (47).

473   Other factors altered by FH in RPE cells include CXCL1/GROα, a chemokine

474   responsible for neutrophil recruitment and activation (48) that has been found increased in

475   aqueous humor of AMD patients (49), and MIP-1α and MIP-1β, which have been found to be

476   involved in inflammation-mediated damage in the retina (50). FH loss in RPE cells also leads

477   to upregulation of IL-1ra, which has been found to be highly expressed by RPE cells in response

478   to IL-1β and TNFα stimulation (51). Interestingly, IL-1β has been found to be highly expressed

479   in iPSC-derived RPE cells carrying the *CFH* 402H variant (52) and TNFα accumulates in the

480   BrM and choroid in eyes from *CFH* 402H donors (53).

481   Our results are in line with independent observations that in AMD, as well as in the

482   presence of the *CFH* 402H variant, inflammation is increased. However, the signaling pathways

483   involved in the regulation of inflammation in RPE cells are not fully characterized, and most

484   importantly the pathway by which FH regulates inflammation in RPE cells was not known. The

485   majority of cytokines differentially regulated in FH-deprived conditions are target of the NF-

486   ƙB pathway. NF-ƙB plays a central role in regulating cellular responses to inflammation and is

487   often activated in concert with the complement system. NF-ƙB consists of transcription factor

488   complexes expressed in most cell types and can be activated in response to a variety of stimuli

489   or stressors, which allow the cell to respond and adapt to variations in the microenvironment

490   including infections, growth factor levels or oxidative stress (32). The most common target

491   genes of the NF-ƙB pathway are inflammatory cytokines, responsible for recruitment of

492   neutrophils and macrophages at the inflamed site (38): cells that are also recruited after local

493   complement activation (17). We have shown here, that NF-ƙB activation follows suppression

494   of *CFH* expression, which in turn results in an upregulation of NF-ƙB dependent cytokines.

495   Reducing NF-ƙB levels leads to a reduction in the expression and secretion of most of the

496   upregulated cytokines, including IL-6, IL-8, CCL2, Serpin E1, GM-CSF and CXCL1/GROα.

497   Consequently, the cytokine profile of the siCFH + siRELA group clusters tightly with the siNeg

498   control.

499   The interaction between the complement system and the NF-ƙB pathway has been

500   reported in other cell types and pathologies, mostly in the context of cell response to

501   complement-mediated damage. Here, NF-ƙB is suggested to play a pro-survival role. Mouse

502   fibroblasts, HELA cells and HEK293 cells lacking NF-ƙB p65, are all more sensitive to

503   complement-mediated damage. Here, the NF-ƙB pathway was found to suppress JNK-

504 dependent programmed necrotic cell death, rather than being involved in complement
505 regulation and inflammation, since no changes in the expression or activity of the complement
506 regulators CD46, CD55 and CD59 were observed (54). Also, HUVEC cells and human
507 coronary endothelial cells (ECs) show NF-ƙB activation in response to MAC formation, in a
508 AKT/endosomes dependent mechanism (55). Data from *in vitro* and *in vivo* models of
509 Alzheimer disease (AD) support the hypothesis that astroglia, rather than neurons, are the
510 principle site of NF-ƙB overactivation and those cells are then primarily responsible for the NF-
511 ƙB -dependent increase in C3. Importantly in this study, NF-ƙB binding sites were confirmed
512 in the *C3* promoter. Moreover, the NF-ƙB /C3 axis in astroglia cells was suggested to be
513 dependent on the classical complement, rather than alternative complement pathway, due to
514 changes in gene expression of C1q and C4 and not Cfb and Cfh (56). Interestingly, HIV
515 infection activates NF-ƙB in astrocytes and promotes C3 production in a IL6-dependent manner
516 (57). Also, results from kidney *in vivo* models of renal injury, provide evidence that the NF-ƙB
517 pathway plays an important role in renal damage mediated by enhanced local complement
518 activation (58).

519 It is important to note that RPE cells, in contrast to all these previously mentioned cell
520 types, show a significant level of tolerance to complement-mediated damage (59). This may
521 explain why they do not exploit the NF-ƙB pathway to respond to external complement
522 stimulation, but rather regulate this pathway to maintain physiological levels of complement
523 and inflammatory factors. Here, the NF-ƙB pathway was not seen activated as pro-survival
524 pathway to respond to a complement activation mediated insult, since addition of neither C3
525 nor C3b had an impact on NF-ƙB activity. However, previous studies have reported that RPE
526 cells show NF-ƙB activation in response to oxidative stress. For instance, ARPE19 cells show
527 increased phosphorylation in NF-ƙB p65 in response to either short or long exposure to H_2O_2
528 (60). In our previous study we show that FH loss increases oxidative and metabolic stress, both
529 stressors of which may induce NF-ƙB activation as a survival mechanism. We have also shown
530 that genes involved in oxidative stress response and mitochondrial stability (*e.g.* PGC1α) were
531 differentially regulated by complement activation: interestingly these are targets of the NF-ƙB
532 pathway as well. Further studies will be necessary to understand the mechanism by which FH
533 loss leads to NF-ƙB activation. Being co-expressed in RPE cells, FH could directly modulate
534 NF-ƙB pathway activation on the protein level. Alternatively, the absence of FH as an
535 antioxidant factor could activate the NF-ƙB pathway in the context of oxidative stress response
536 in RPE cells.

537   The observation, that a subset of cytokines (MIP-1α, MIP-1β and IL-1ra), which were

538   increased upon FH loss, were not reduced after silencing of NF-ƙB p65 suggests, that additional

539   pathways are likely involved in the interplay between complement and NF-ƙB pathway. Several

540   pathways have been described as being involved in the homeostasis of RPE cells, which could

541   be regulated by FH. For example, knock-out of CXCR5 in RPE cells leads to an AMD-like

542   phenotype and transcriptome profile highlights the role of PI3K-Akt and mTOR signaling, as

543   important pathways for RPE homeostasis (61). Another possibility involves the regulation of

544   the transcription factor AP1, which has been found to be regulated together with NF-ƙB in

545   response to blue-light mediated damage (62).

546   Although the exact mechanism remains to be discovered, our data contribute to the

547   understanding around how risk alleles in *CFH* which result in reduced FH/FHL-1 activity may

548   increase the risk for AMD. We suggest that in RPE cells, FH and the NF-ƙB pathway work in

549   synergy to maintain cellular homeostasis, keeping both pro-inflammatory pathways in balance

550   and check (summarized in Fig. 5). In case either one of them is dysregulated due to genetic risk,

551   age and/or local stressors, the RPE microenvironment changes towards a pro-inflammatory

552   AMD-like phenotype, with NF-ƙB as well as the alternative complement pathway acting as

553   major protagonists.

554
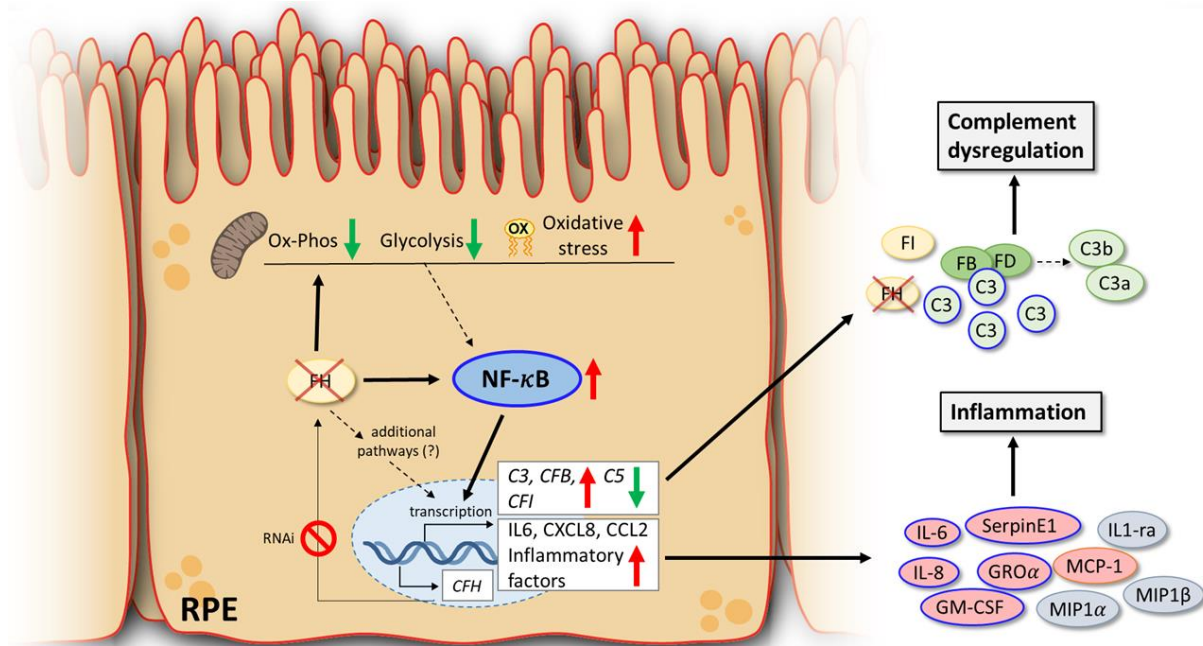
Figure 5. Summary schematic of NF-kB-mediated inflammation driven by the loss of CFH. Reduced levels of *CFH* via RNAi in RPE cells leads to activation of the NF-κB pathway (blue). The NF-κB pathway regulates gene transcription of inflammatory cytokines (light red) as well as positive (green) and negative (yellow) regulators of complement activation, secreted from RPE. FH-deprived RPE cells are characterized by reduced levels of oxidative phosphorylation (Ox-Phos) and glycolysis, as well as increased oxidative stress and oxidized lipids levels (ox). Metabolic and oxidative stresses are known positive regulators of the NF-κB pathway and could contribute to the activation of the NF-κB pathway in FH-reduced conditions (dotted arrow). Secreted proteins circled in blue are directly modulated through the actions of the NFkB pathway. Cytokines secreted in FH-deprived RPE cells, which are not regulated by NF-κB pathway, are labeled grey.

References

1. Zhou, R., and R. R. Caspi. 2010. Ocular immune privilege. *F1000 biology reports* 2.

2. Curcio, C. A., and M. Johnson. 2013. Chapter 20 - Structure, Function, and Pathology of Bruch's Membrane. In *Retina (Fifth Edition)*. S. J. Ryan, S. R. Sadda, D. R. Hinton, A. P. Schachat, S. R. Sadda, C. P. Wilkinson, P. Wiedemann, and A. P. Schachat, eds. W.B. Saunders, London. 465-481.

3. Clark, S. J., S. McHarg, V. Tilakaratna, N. Brace, and P. N. Bishop. 2017. Bruch's Membrane Compartmentalizes Complement Regulation in the Eye with Implications for Therapeutic Design in Age-Related Macular Degeneration. *Front Immunol* 8: 1778.

4. Strauss, O. 2005. The retinal pigment epithelium in visual function. *Physiol Rev* 85: 845-881.

5. Rashid, K., I. Akhtar-Schaefer, and T. Langmann. 2019. Microglia in Retinal Degeneration. *Front Immunol* 10: 1975.

6. van Lookeren Campagne, M., J. LeCouter, B. L. Yaspan, and W. Ye. 2014. Mechanisms of age-related macular degeneration and therapeutic opportunities. *The Journal of Pathology* 232: 151-164.

7. Handa, J. T., C. Bowes Rickman, A. D. Dick, M. B. Gorin, J. W. Miller, C. A. Toth, M. Ueffing, M. Zarbin, and L. A. Farrer. 2019. A systems biology approach towards understanding and treating non-neovascular age-related macular degeneration. *Nat Commun* 10: 3347.

8. Klein, R., T. Peto, A. Bird, and M. R. Vannewkirk. 2004. The epidemiology of age-related macular degeneration. *Am J Ophthalmol* 137: 486-495.

9. Mullins, R. F., S. R. Russell, D. H. Anderson, and G. S. Hageman. 2000. Drusen associated with aging and age-related macular degeneration contain proteins common to extracellular deposits associated with atherosclerosis, elastosis, amyloidosis, and dense deposit disease. *FASEB J* 14: 835-846.

10. Priya, R. R., E. Y. Chew, and A. Swaroop. 2012. Genetic studies of age-related macular degeneration: lessons, challenges, and opportunities for disease management. *Ophthalmology* 119: 2526-2536.

11. Ajana, S., A. Cougnard-Gregoire, J. M. Colijn, B. M. J. Merle, T. Verzijden, P. de Jong, A. Hofman, J. R. Vingerling, B. P. Hejblum, J. F. Korobelnik, M. A. Meester-Smoor, M. Ueffing, H. Jacqmin-Gadda, C. C. W. Klaver, C. Delcourt, and E.-R. Consortium. 2020. Predicting Progression to Advanced Age-Related Macular Degeneration from Clinical, Genetic, and Lifestyle Factors Using Machine Learning. *Ophthalmology*.

12. Heesterbeek, T. J., L. Lorés-Motta, C. B. Hoyng, Y. T. E. Lechanteur, and A. I. den Hollander. 2020. Risk factors for progression of age-related macular degeneration. *Ophthalmic Physiol Opt* 40: 140-170.

13. Fritsche, L. G., R. N. Fariss, D. Stambolian, G. R. Abecasis, C. A. Curcio, and A. Swaroop. 2014. Age-related macular degeneration: genetics and biology coming together. *Annu Rev Genomics Hum Genet* 15: 151-171.

14. Ricklin, D., G. Hajishengallis, K. Yang, and J. D. Lambris. 2010. Complement: a key system for immune surveillance and homeostasis. *Nature immunology* 11: 785-797.

15. Streilein, J. W. 2003. Ocular immune privilege: the eye takes a dim but practical view of immunity and inflammation. *J Leukoc Biol* 74: 179-185.

16. Klos, A., A. J. Tenner, K. O. Johswich, R. R. Ager, E. S. Reis, and J. Kohl. 2009. The role of the anaphylatoxins in health and disease. *Mol Immunol* 46: 2753-2766.

17. Behnke, V., A. Wolf, and T. Langmann. 2020. The role of lymphocytes and phagocytes in age-related macular degeneration (AMD). *Cell Mol Life Sci* 77: 781-788.

18. Tan, W., J. Zou, S. Yoshida, B. Jiang, and Y. Zhou. 2020. The Role of Inflammation in Age-Related Macular Degeneration. *International journal of biological sciences* 16: 2989-3001.

19. Heesterbeek, T. J., Y. T. E. Lechanteur, L. Lores-Motta, T. Schick, M. R. Daha, L. Altay, S. Liakopoulos, D. Smailhodzic, A. I. den Hollander, C. B. Hoyng, E. K. de Jong, and B. J. Klevering. 2020. Complement Activation Levels Are Related to Disease Stage in AMD. *Invest Ophthalmol Vis Sci* 61: 18.

619   20.   Keenan, T. D., M. Toso, C. Pappas, L. Nichols, P. N. Bishop, and G. S. Hageman. 2015.
620   Assessment of Proteins Associated With Complement Activation and Inflammation in
621   Maculae of Human Donors Homozygous Risk at Chromosome 1 CFH-to-F13B. *Invest*
622   *Ophthalmol Vis Sci* 56: 4870-4879.
623   21.   Edwards, A. O., R. Ritter, 3rd, K. J. Abel, A. Manning, C. Panhuysen, and L. A. Farrer. 2005.
624   Complement factor H polymorphism and age-related macular degeneration. *Science* 308:
625   421-424.
626   22.   Day, A. J., A. C. Willis, J. Ripoche, and R. B. Sim. 1988. Sequence polymorphism of human
627   complement factor H. *Immunogenetics* 27: 211-214.
628   23.   Clark, S. J., C. Q. Schmidt, A. M. White, S. Hakobyan, B. P. Morgan, and P. N. Bishop. 2014.
629   Identification of factor H-like protein 1 as the predominant complement regulator in Bruch's
630   membrane: implications for age-related macular degeneration. *J Immunol* 193: 4962-4970.
631   24.   Armento, A., M. Ueffing, and S. J. Clark. 2021. The complement system in age-related
632   macular degeneration. *Cellular and Molecular Life Sciences*.
633   25.   Skerka, C., N. Lauer, A. A. Weinberger, C. N. Keilhauer, J. Suhnel, R. Smith, U. Schlotzer-
634   Schrehardt, L. Fritsche, S. Heinen, A. Hartmann, B. H. Weber, and P. F. Zipfel. 2007. Defective
635   complement control of factor H (Y402H) and FHL-1 in age-related macular degeneration. *Mol*
636   *Immunol* 44: 3398-3406.
637   26.   Clark, S. J., R. Perveen, S. Hakobyan, B. P. Morgan, R. B. Sim, P. N. Bishop, and A. J. Day. 2010.
638   Impaired binding of the age-related macular degeneration-associated complement factor H
639   402H allotype to Bruch's membrane in human retina. *J Biol Chem* 285: 30192-30202.
640   27.   Shaw, P. X., L. Zhang, M. Zhang, H. Du, L. Zhao, C. Lee, S. Grob, S. L. Lim, G. Hughes, J. Lee, M.
641   Bedell, M. H. Nelson, F. Lu, M. Krupa, J. Luo, H. Ouyang, Z. Tu, Z. Su, J. Zhu, X. Wei, Z. Feng, Y.
642   Duan, Z. Yang, H. Ferreyra, D. U. Bartsch, I. Kozak, L. Zhang, F. Lin, H. Sun, H. Feng, and K.
643   Zhang. 2012. Complement factor H genotypes impact risk of age-related macular
644   degeneration by interaction with oxidized phospholipids. *Proc Natl Acad Sci U S A* 109:
645   13757-13762.
646   28.   Molins, B., P. Fuentes-Prior, A. Adan, R. Anton, J. I. Arostegui, J. Yague, and A. D. Dick. 2016.
647   Complement factor H binding of monomeric C-reactive protein downregulates
648   proinflammatory activity and is impaired with at risk polymorphic CFH variants. *Sci Rep* 6:
649   22889.
650   29.   Swinkels, M., J. H. Zhang, V. Tilakaratna, G. Black, R. Perveen, S. McHarg, A. Inforzato, A. J.
651   Day, and S. J. Clark. 2018. C-reactive protein and pentraxin-3 binding of factor H-like protein
652   1 differs from complement factor H: implications for retinal inflammation. *Sci Rep* 8: 1643.
653   30.   Mannes, M., A. Dopler, M. Huber-Lang, and C. Q. Schmidt. 2020. Tuning the Functionality by
654   Splicing: Factor H and Its Alternative Splice Variant FHL-1 Share a Gene but Not All Functions.
655   *Frontiers in Immunology* 11.
656   31.   Armento, A., S. Honisch, V. Panagiotakopoulou, I. Sonntag, A. Jacob, S. Bolz, E. Kilger, M.
657   Deleidi, S. Clark, and M. Ueffing. 2020. Loss of Complement Factor H impairs antioxidant
658   capacity and energy metabolism of human RPE cells. *Sci Rep* 10: 10320.
659   32.   Oeckinghaus, A., and S. Ghosh. 2009. The NF-kappaB family of transcription factors and its
660   regulation. *Cold Spring Harbor perspectives in biology* 1: a000034.
661   33.   Singh, S., and T. G. Singh. 2020. Role of Nuclear Factor Kappa B (NF-kappaB) Signalling in
662   Neurodegenerative Diseases: An Mechanistic Approach. *Curr Neuropharmacol* 18: 918-935.
663   34.   Steinle, J. J. 2020. Role of HMGB1 signaling in the inflammatory process in diabetic
664   retinopathy. *Cellular signalling* 73: 109687.
665   35.   Pang, Z., J. Chong, S. Li, and J. Xia. 2020. MetaboAnalystR 3.0: Toward an Optimized
666   Workflow for Global Metabolomics. *Metabolites* 10: 186.
667   36.   Macchioni, L., D. Chiasserini, L. Mezzasoma, M. Davidescu, P. L. Orvietani, K. Fettucciari, L.
668   Salviati, B. Cellini, and I. Bellezza. 2020. Crosstalk between Long-Term Sublethal Oxidative
669   Stress and Detrimental Inflammation as Potential Drivers for Age-Related Retinal
670   Degeneration. *Antioxidants (Basel)* 10.

671   37.   Kim, S. Y., S. P. Kambhampati, I. A. Bhutto, D. S. McLeod, G. A. Lutty, and R. M. Kannan. 2021.
672   Evolution of oxidative stress, inflammation and neovascularization in the choroid and retina
673   in a subretinal lipid induced age-related macular degeneration model. *Exp Eye Res* 203:
674   108391.
675   38.   Mitchell, S., J. Vargas, and A. Hoffmann. 2016. Signaling via the NFκB system. *Wiley*
676   *interdisciplinary reviews. Systems biology and medicine* 8: 227-241.
677   39.   Marazita, M. C., A. Dugour, M. D. Marquioni-Ramella, J. M. Figueroa, and A. M. Suburo. 2016.
678   Oxidative stress-induced premature senescence dysregulates VEGF and CFH expression in
679   retinal pigment epithelial cells: Implications for Age-related Macular Degeneration. *Redox*
680   *Biol* 7: 78-87.
681   40.   Nahavandipour, A., M. Krogh Nielsen, T. L. Sørensen, and Y. Subhi. 2020. Systemic levels of
682   interleukin-6 in patients with age-related macular degeneration: a systematic review and
683   meta-analysis. *Acta Ophthalmol*.
684   41.   Wang, S., C. Liu, W. Ouyang, Y. Liu, C. Li, Y. Cheng, Y. Su, C. Liu, L. Yang, Y. Liu, and Z. Wang.
685   2021. Common Genes Involved in Autophagy, Cellular Senescence and the Inflammatory
686   Response in AMD and Drug Discovery Identified via Biomedical Databases. *Transl Vis Sci*
687   *Technol* 10: 14.
688   42.   Crane, I. J., M. C. Kuppner, S. McKillop-Smith, C. A. Wallace, and J. V. Forrester. 1999.
689   Cytokine regulation of granulocyte-macrophage colony-stimulating factor (GM-CSF)
690   production by human retinal pigment epithelial cells. *Clin Exp Immunol* 115: 288-293.
691   43.   Wang, J. C. C., S. Cao, A. Wang, E. To, G. Law, J. Gao, D. Zhang, J. Z. Cui, and J. A. Matsubara.
692   2015. CFH Y402H polymorphism is associated with elevated vitreal GM-CSF and choroidal
693   macrophages in the postmortem human eye. In *Molecular vision*. 264-272.
694   44.   Vaughan, D. E., R. Rai, S. S. Khan, M. Eren, and A. K. Ghosh. 2017. Plasminogen Activator
695   Inhibitor-1 Is a Marker and a Mediator of Senescence. *Arterioscler Thromb Vasc Biol* 37:
696   1446-1452.
697   45.   Lambert, V., C. Munaut, A. Noël, F. Frankenne, K. Bajou, R. Gerard, P. Carmeliet, M. P.
698   Defresne, J. M. Foidart, and J. M. Rakic. 2001. Influence of plasminogen activator inhibitor
699   type 1 on choroidal neovascularization. *Faseb j* 15: 1021-1027.
700   46.   Stefansson, S., and D. A. Lawrence. 1996. The serpin PAI-1 inhibits cell migration by blocking
701   integrin αvβ3 binding to vitronectin. *Nature* 383: 441-443.
702   47.   Choudhury, R., N. Bayatti, R. Scharff, E. Szula, V. Tilakaratna, M. S. Udsen, S. McHarg, J. A.
703   Askari, M. J. Humphries, P. N. Bishop, and S. J. Clark. 2020. FHL-1 interacts with human RPE
704   cells through the α5β1 integrin and confers protection against oxidative stress. *bioRxiv*:
705   2020.2009.2028.317263.
706   48.   Sawant, K. V., K. M. Poluri, A. K. Dutta, K. M. Sepuru, A. Troshkina, R. P. Garofalo, and K.
707   Rajarathnam. 2016. Chemokine CXCL1 mediated neutrophil recruitment: Role of
708   glycosaminoglycan interactions. *Scientific Reports* 6: 33123.
709   49.   Agrawal, R., P. K. Balne, X. Wei, V. A. Bijin, B. Lee, A. Ghosh, R. Narayanan, M. Agrawal, and J.
710   Connolly. 2019. Cytokine Profiling in Patients With Exudative Age-Related Macular
711   Degeneration and Polypoidal Choroidal Vasculopathy. *Investigative Ophthalmology & Visual*
712   *Science* 60: 376-382.
713   50.   Rutar, M., R. Natoli, R. X. Chia, K. Valter, and J. M. Provis. 2015. Chemokine-mediated
714   inflammation in the degenerating retina is coordinated by Müller cells, activated microglia,
715   and retinal pigment epithelium. *Journal of Neuroinflammation* 12: 8.
716   51.   Sugita, S., Y. Kawazoe, A. Imai, Y. Usui, Y. Iwakura, K. Isoda, M. Ito, and M. Mochizuki. 2013.
717   Mature dendritic cell suppression by IL-1 receptor antagonist on retinal pigment epithelium
718   cells. *Invest Ophthalmol Vis Sci* 54: 3240-3249.
719   52.   Hallam, D., J. Collin, S. Bojic, V. Chichagova, A. Buskin, Y. Xu, L. Lafage, E. G. Otten, G.
720   Anyfantis, C. Mellough, S. Przyborski, S. Alharthi, V. Korolchuk, A. Lotery, G. Saretzki, M.
721   McKibbin, L. Armstrong, D. Steel, D. Kavanagh, and M. Lako. 2017. An Induced Pluripotent
722   Stem Cell Patient Specific Model of Complement Factor H (Y402H) Polymorphism Displays

723   Characteristic Features of Age-Related Macular Degeneration and Indicates a Beneficial Role
724   for UV Light Exposure. *Stem Cells* 35: 2305-2320.

725   53.   Cao, S., J. C. Wang, J. Gao, M. Wong, E. To, V. A. White, J. Z. Cui, and J. A. Matsubara. 2016.
726   CFH Y402H polymorphism and the complement activation product C5a: effects on NF-kappaB
727   activation and inflammasome gene regulation. *Br J Ophthalmol* 100: 713-718.

728   54.   Gancz, D., M. Lusthaus, and Z. Fishelson. 2012. A Role for the NF-κB Pathway in Cell
729   Protection from Complement-Dependent Cytotoxicity. *The Journal of Immunology* 189: 860-
730   866.

731   55.   Jane-wit, D., Y. V. Surovtseva, L. Qin, G. Li, R. Liu, P. Clark, T. D. Manes, C. Wang, M.
732   Kashgarian, N. C. Kirkiles-Smith, G. Tellides, and J. S. Pober. 2015. Complement membrane
733   attack complexes activate noncanonical NF-κB by forming an Akt$^+$/NIK$^+$/signalosome on
734   Rab5$^+$ endosomes. *Proceedings of the National Academy of Sciences* 112: 9686-9691.

735   56.   Lian, H., L. Yang, A. Cole, L. Sun, A. C. Chiang, S. W. Fowler, D. J. Shim, J. Rodriguez-Rivera, G.
736   Taglialatela, J. L. Jankowsky, H. C. Lu, and H. Zheng. 2015. NFkappaB-activated astroglial
737   release of complement C3 compromises neuronal morphology and function associated with
738   Alzheimer's disease. *Neuron* 85: 101-115.

739   57.   Nitkiewicz, J., A. Borjabad, S. Morgello, J. Murray, W. Chao, L. Emdad, P. B. Fisher, M. J.
740   Potash, and D. J. Volsky. 2017. HIV induces expression of complement component C3 in
741   astrocytes by NF-κB-dependent activation of interleukin-6 synthesis. *Journal of
742   Neuroinflammation* 14: 23.

743   58.   Liu, M., H. Wang, J. Zhang, X. Yang, B. Li, C. Wu, and Q. Zhu. 2018. NF-κB signaling pathway-
744   enhanced complement activation mediates renal injury in trichloroethylene-sensitized mice.
745   *Journal of Immunotoxicology* 15: 63-72.

746   59.   Whitmore, S. S., E. H. Sohn, K. R. Chirco, A. V. Drack, E. M. Stone, B. A. Tucker, and R. F.
747   Mullins. 2015. Complement activation and choriocapillaris loss in early AMD: implications for
748   pathophysiology and therapy. *Prog Retin Eye Res* 45: 1-29.

749   60.   Song, C., S. K. Mitter, X. Qi, E. Beli, H. V. Rao, J. Ding, C. S. Ip, H. Gu, D. Akin, W. A. Dunn, Jr., C.
750   Bowes Rickman, A. S. Lewin, M. B. Grant, and M. E. Boulton. 2017. Oxidative stress-mediated
751   NFkappaB phosphorylation upregulates p62/SQSTM1 and promotes retinal pigmented
752   epithelial cell survival through increased autophagy. *PLoS One* 12: e0171940.

753   61.   Saddala, M. S., A. Lennikov, A. Mukwaya, and H. Huang. 2020. Transcriptome-Wide Analysis
754   of CXCR5 Deficient Retinal Pigment Epithelial (RPE) Cells Reveals Molecular Signatures of RPE
755   Homeostasis. *Biomedicines* 8.

756   62.   Kim, J., H. L. Jin, D. S. Jang, K. W. Jeong, and S. Y. Choung. 2018. Quercetin-3-O-α-l-
757   arabinopyranoside protects against retinal cell death via blue light-induced damage in human
758   RPE cells and Balb-c mice. *Food Funct* 9: 2171-2183.

759